

4-2016

# Ion transport through macrocapillaries – Oscillations due to charge patch formation

Dhruva Kulkarni

*Clemson University, [dkulkar@clemson.edu](mailto:dkulkar@clemson.edu)*

L.A.M. Lyle

*University at Buffalo, The State University of New York*

Chad E. Sosolik

*Clemson University*

Follow this and additional works at: [https://tigerprints.clemson.edu/physastro\\_pubs](https://tigerprints.clemson.edu/physastro_pubs)



Part of the [Astrophysics and Astronomy Commons](#), and the [Physics Commons](#)

---

## Recommended Citation

Please use the publisher's recommended citation: <http://www.sciencedirect.com/science/article/pii/S0168583X16300817>

This Article is brought to you for free and open access by the Physics and Astronomy at TigerPrints. It has been accepted for inclusion in Publications by an authorized administrator of TigerPrints. For more information, please contact [kokeefe@clemson.edu](mailto:kokeefe@clemson.edu).

# Ion transport through macrocapillaries - oscillations due to charge patch formation

D.D. Kulkarni<sup>a</sup>, L.A.M. Lyle<sup>b</sup>, C.E. Sosolik<sup>a,\*</sup>

<sup>a</sup>*Department of Physics and Astronomy, Clemson University, Clemson, South Carolina, 29634 USA*

<sup>b</sup>*Department of Physics, University at Buffalo, The State University of New York, Buffalo, NY 14260, USA*

---

## Abstract

We present results on ion transport through large bore capillaries (macrocapillaries) that probe both the geometric and ion-guided aspects of this ion delivery mechanism. We have demonstrated that guiding in macrocapillaries exhibits position- and angle-dependent transmission properties which are directly related to the capillary material (either metal or insulator) and geometry. Specifically, we have passed 1 keV Rb<sup>+</sup> ions through glass and metal macrocapillaries, and have observed oscillations for the transmitted ion current passing through the insulating capillaries. Straightforward calculations show that these oscillations can be attributed to beam deflections from charge patches that form on the interior walls of the capillary. The absence of these oscillations in the metal capillary data serve as further confirmation of the role of charge patch formation.

---

## 1. Introduction

1           Multiply/Highly charged ions (M/HCIs) are unique in the field of ion-related physics  
2           as their charge state is significantly higher than the traditional singly-charged ions  
3           which dominate the field. This charge state, which is manifest as a non-negligible  
4           potential energy of the ions, can be used to modify the surface/subsurface structure  
5           of materials in ways that are distinct from other forms of radiation[1–6]. Beams of  
6           M/HCIs are obtained from sources such as Electron Beam Ion Source/Traps (EBIS/Ts)  
7           and Electron Cyclotron Resonance (ECR) ion sources in laboratories worldwide[7–14]  
8           and most recently at our own user facility for surface modification[15] as well as med-  
9           ical physics[16]. Despite this access, a major hurdle in effectively harnessing the po-  
10          tential of these beams for industrial environments is efficient and flexible ion-transport  
11          technology.

12           One approach towards non-conventional ion transport that has garnered significant  
13          attention over the last two decades is the use of capillaries as ion guides. In 2002,  
14          Stolterfoht *et al.* observed the so-called "guiding effect" in insulating capillaries[17].  
15

---

\*Corresponding author

*Email address:* sosolik@clemson.edu (C.E. Sosolik)

1 This effect involves charge patch formation on the inside walls of the insulating capil-  
2 lary due to neutralization of and secondary electron emission initiated by the colliding  
3 M/HCI beam. Although these charges formed on the wall can dissipate into the capil-  
4 lary bulk or along the surface, they can also interact repulsively with ions of the incom-  
5 ing M/HCI beam to deflect them away from the capillary wall. After sufficient time has  
6 elapsed, a steady-state condition can be reached between charge patch formation and  
7 charge dissipation such that a charge-state and kinetic energy preserving transmission  
8 of the M/HCI beam is established. This is the definition of the guiding effect for ions  
9 within a capillary, and an extensive review of the existing research in this field can be  
10 found in Ref. [18].

11 Existing research can be classified into two categories depending on the diameter  $d$   
12 of the capillaries used for guiding: nanocapillaries ( $d < 1 \mu\text{m}$ ) and macrocapillar-  
13 ies ( $d > 1 \mu\text{m}$ )[19]. Recent efforts in macrocapillary transport include the use of ex-  
14 ternal electric fields to guide the ions in conjunction with the guiding effect to improve  
15 efficiency of transport[20], use of conical capillaries for guiding antiparticle beams[21]  
16 and the use of curved glass capillaries to achieve large bending angles[22]. In this pa-  
17 per, we have studied the transport of singly-charged ions through straight and conical  
18 sections of insulating as well as metallic macrocapillaries. Our goal was to measure and  
19 understand the position- and angle-dependent characteristics of ion transport through  
20 these macrocapillaries.

21 The organization of this paper is as follows. In Sec. 2 we describe the experimental  
22 setup used in these measurements. In Sec. 3, we present data measured on a cylindrical  
23 metallic, a cylindrical insulating and a conical insulating macrocapillary. Differences  
24 and similarities in the data are noted and used to draw conclusions regarding charging  
25 effects, which are summarized in Sec. 4.

## 26 2. Experiment

27 We have measured the position- and angle-dependent transmission properties of  
28 singly-charged ions for macrocapillaries with diameters and lengths of a few millime-  
29 ters and a few centimeters respectively. The experiment was conducted at Clemson  
30 University using the singly charged ion beamline described in detail in Ref. [23]. An  
31 aluminosilicate emitter (HeatWave Labs, Inc.) was installed as the ion source in the  
32 beamline to obtain  $\text{Rb}^+$  ions. The kinetic energy of the  $\text{Rb}^+$  ions was fixed at 1 keV for  
33 all measurements. The energy spread of the beam is less than 1 % [24].

34 Macrocapillaries of two types were used in this study: metals (stainless steel) and  
35 insulators (glass). The dimensions of the capillaries are shown in Table 1. The inlet  
36 refers to the side of the capillary through which the ions were incident, while the outlet  
37 is the exit side of the capillary. The critical angle  $\theta_c$  is defined as the maximum angle  
38 of the capillary with respect to the incident beam of ions for which geometric trans-  
39 mission is possible. This angle is equivalent to the angle made by a line that touches  
40 the farthest and opposite corners in a length-wise cross-section of a capillary and is  
41 given by  $\theta_c = \tan^{-1}((d_{in} + d_{out}) / 2l)$ . We note that for our study, all capillaries were  
42 cylindrical ( $d_{in} = d_{out}$ ) except one conical capillary denoted by Sample # 4 which had  
43 a taper of  $4.52^\circ \pm 0.12^\circ$ .

Table 1: Table showing the material, length ( $l$ ), inlet diameter ( $d_{in}$ ), outlet diameter ( $d_{out}$ ) and critical angle ( $\theta_c$ ) for the various macrocapillaries used in this experiment. The uncertainties associated with these dimensions are  $\pm 0.1$  mm and  $\pm 0.12^\circ$ .

Sample #	Material	$l$ (mm)	$d_{in}$ (mm)	$d_{out}$ (mm)	$\theta_c$ ( $^\circ$ )
1	Steel	21.0	2.3	2.3	6.25
2	Glass	35.5	5.4	5.4	8.65
3	Glass	21.0	5.4	5.4	14.42
4	Glass	19.6	5.4	2.3	11.11

1 Before inserting the capillaries into our vacuum system, they were cleaned using  
2 standard UHV procedures, i.e. ten minute cycles of sonication with soap-water, ace-  
3 tone, and ethanol interspersed with rinsing in distilled water. Each macrocapillary was  
4 then mounted in a custom vacuum chamber inserted immediately after our Colutron  
5 G2 ion source[25]. The typical pressure in the chamber for these measurements was  
6  $\sim 1 \times 10^{-8}$  Torr. The macrocapillaries were secured along the beamline axis on a ro-  
7 tary feedthrough mounted on a linear translator. The translator allowed us to move the  
8 capillary perpendicular to the path of the beam to measure position dependent charac-  
9 teristics, while the rotary feedthrough allowed us to change the incident angle of the  
10 incoming ions relative to the capillary inlet. Each capillary was mounted with an adhe-  
11 sive metal tape on the exposed edge of the inlet to avoid entrance charging effects. The  
12 space around the capillary was shielded using a metal foil held in place by metal adhe-  
13 sive tape. The shield was necessary to ensure that only those ions that passed through  
14 the inside of the capillary and not around it were detected in these measurements.

15 A Faraday cup located  $\sim 15$  cm downstream from the capillary mounting was used  
16 to measure the current of ions transmitted through the capillaries. For each measure-  
17 ment, the  $\text{Rb}^+$  ion beam was tuned into the Faraday cup with the capillary retracted  
18 from the beam path. The capillary was then inserted into the path of the beam and the  
19 cup current was monitored to determine the insertion distance at which transmission  
20 of ions through the capillary was maximized. In addition, the insertion distances (on  
21 either side of this maximum point) at which the measured transmission through the  
22 capillary was zero were also recorded. Following these baseline measurements, the  
23 transmitted current was monitored as a function of time at multiple distances between  
24 the zero measurement end-points to obtain position-dependent characteristics (see, *e.g.*  
25 Fig. 1a). Angle-dependent characteristics for each capillary were obtained at the inser-  
26 tion distance of maximum transmission by varying the angle in steps of  $\sim 0.2^\circ - 0.3^\circ$  and  
27 monitoring the transmitted current as a function of time (see, *e.g.* Fig 1b). For these  
28 position- and angle-dependent measurements, the transmitted current through the metal  
29 and insulating capillaries was recorded in time steps of  $\sim 15$  seconds and  $\sim 500$  seconds  
30 respectively. Insertion distances were measured using a Vernier caliper ( $\pm 0.1$  mm),  
31 while a digital sensor connected to a PC was used to measure angles ( $\pm 0.09^\circ$ ). The  
32 Faraday cup was connected to a Keithley 617 electrometer interfaced to a computer via  
33 GPIB for automated measurements. To improve the current measurement precision,  
34 the connection points for the Faraday cup were sanded down and connected using ex-  
35 tremely short cables to reduce capacitive losses and the electrometer power connection

1 was isolated from other laboratory connections to minimize AC pick-up. These steps  
 2 resulted in a precision of  $\pm 5$  pA for our measurements of transmitted current.

### 3 3. Results and Discussion

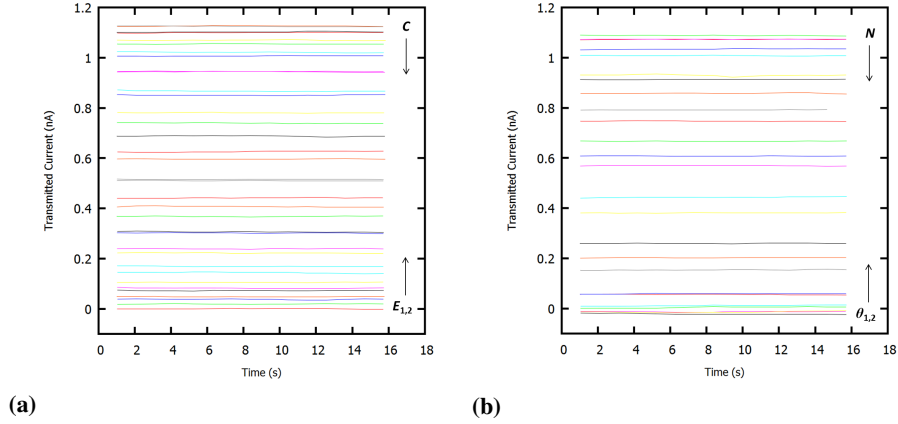


Figure 1: [Color Online] a) Position- and b) angle-dependent raw data for the metal capillary (Sample # 1,  $l=2.10$  cm,  $d_{in}=d_{out}=0.23$  cm). The transmitted current is plotted as a function of time at varying positions and angles. See text for details.

4 Position- and angle-dependent data were obtained for the four macrocapillaries  
 5 listed in Table 1 using the methods described in the previous section. Figure 1 shows  
 6 transmitted currents as a function of time measured for the metal capillary (Sample # 1).  
 7 Each line in the figure refers to a measurement conducted when the capillary was in-  
 8 serted to a specific distance (Fig. 1a) or rotated to a specific angle (Fig. 1b) in the  
 9 presence of the incident ion beam. In Fig. 1a, the positions  $E_1$ ,  $E_2$ , and  $C$  refer to the  
 10 insertion distances where the transmitted ion current through the capillary are zero ( $E_1$   
 11 and  $E_2$ ) or maximum ( $C$ ). The up and down arrows in the figure indicate that as the  
 12 capillary was moved away from the  $E_1/E_2$  position or the  $C$  position, the transmitted  
 13 current increased or decreased, respectively. For this metal macrocapillary these posi-  
 14 tions were  $(E_1, E_2, C) = (0.0$  mm,  $14.4$  mm,  $7.2$  mm). These data indicate that the  
 15 width of the incident ion beam was  $\sim 14$  mm, which is much wider than the diameter  
 16 of all of the capillaries used in this study. For the angular data shown in Fig. 1b,  $\theta_{1,2}$   
 17 refer to the angles at which transmission dropped to zero while  $N$  refers to maximum  
 18 transmission observed at normal incidence. As with the insertion data, the arrows on  
 19 this figure refer to the increase or decrease of the transmitted current for rotations of  
 20 the angle away from or toward the positions  $\theta_{1,2}$  and  $N$ . For this metal macrocapillary  
 21 the zero transmission angles were  $(\theta_1, \theta_2)=(-6.12^\circ, 7.02^\circ)$ , which lead to a measured  
 22 critical angle  $\theta_c=6.57\pm 0.09$  as compared to the theoretical value of  $6.25^\circ$ .

23 For the angular data of Fig. 1b, the maximum, minimum and mean transmitted  
 24 current values measured at each angle were calculated and are plotted in Fig. 2. For  
 25 this metal macrocapillary, these values are nearly equivalent and the plotted data lie on

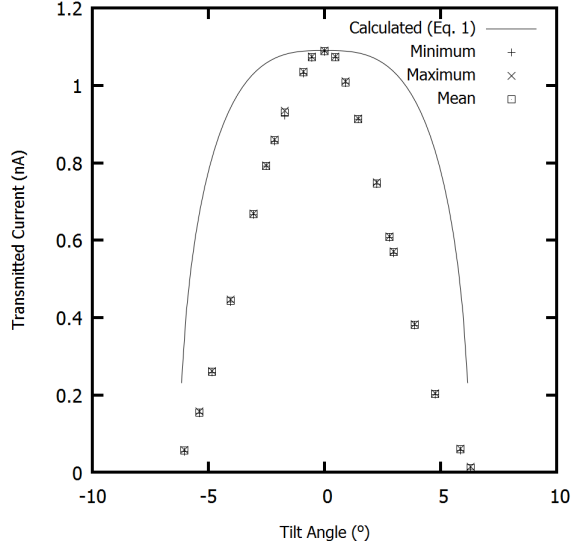


Figure 2: Maximum, mean and minimum of transmitted current as a function of varying tilt angle for the metal capillary (Sample # 1,  $l=2.10$  cm,  $d_{in}=d_{out}=0.23$  cm). The line shows the expected geometrical transmission from the capillary as a function of tilt angle.

1 top of each other in the figure. For the glass capillaries (discussed below) this will no  
 2 longer be the case. To understand the angular dependence shown in these data, we note  
 3 that the tilt of the capillary modifies the effective opening area presented to the incident  
 4 beam, as illustrated in Fig. 3 for a capillary of diameter  $d$  and length  $l$ . The functional  
 5 form of this angular-dependent area,  $A(\theta)$ , is given by

$$A(\theta) = \frac{d^2}{2} \cos(\theta) [-\sin^{-1}(\gamma) + \gamma \cos(\sin^{-1}(\gamma)) + \pi/2] \quad (1)$$

6 where  $\gamma = (l/d)\tan(\theta)$ .

7 The solid line in Fig. 2, which corresponds to this equation for our metal macro-  
 8 capillary, shows that the measured angular-dependence of the transmitted current has  
 9 a narrower angular range than this calculated geometrical limit. We note that our as-  
 10 sumption of a constant current density and zero divergence for our incident ion beam  
 11 could give rise to this discrepancy between the measured and calculated transmission  
 12 values. For example, a Gaussian current density convolved with the functional form  
 13 for  $A(\theta)$  along with losses due to divergence would decrease the angular range of the  
 14 calculated transmission. These corrections, which require more detailed incident ion  
 15 beam measurements, will be pursued in future measurements.

16 Representative data for a straight glass macrocapillary (Sample # 2) is shown in  
 17 Figs. 4 and 5. A comparison of the time-dependent results for the both the position  
 18 (Fig. 4a) and tilt angle (Fig. 4b) with those discussed above for the the metal macro-  
 19 capillary (Fig. 1) reveals the primary difference between these capillary types, which  
 20 is the oscillations in the transmitted current for the glass macrocapillary. Specifically,

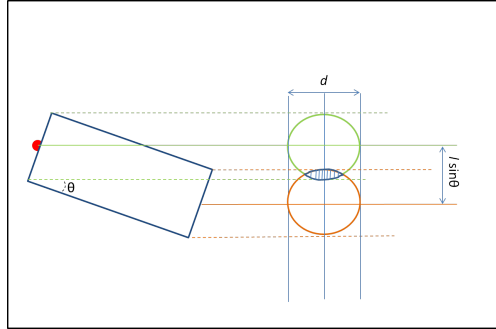


Figure 3: [Color Online] Figure illustrating the varying area of the effective opening (hatched) as the capillary is tilted by an angle  $\theta$  resulting in the observed angle-dependent characteristics for geometric transmission. An exact expression for this dependence is shown in Eq. 1 of the text.

1 within the measurement ranges of  $E_{1,2}$  and  $\theta_{1,2}$  there are significant, time-dependent  
 2 excursions in the transmitted current on a timescale of approximately one second. We  
 3 note that the incident beam conditions for these capillary types (metal vs. insulating)  
 4 was similar, which can be verified by examining the beam width and maximum trans-  
 5 mitted current across the various measurements. For example, for these Sample # 2  
 6 data we obtained an ion beam width of  $\sim 14$  mm, which is similar to the beam width  
 7 determined for the metal macrocapillary (Sample # 1). In addition, the ratio of the max-  
 8 imum transmitted current in the metal and insulating capillaries ( $\sim 5.48$ ) is close to the  
 9 ratio of the inlet area of the two capillaries ( $\sim 5.51$ ). Similar results were found for the  
 10 other macrocapillaries listed in Table 1. Therefore, we conclude that the transmitted  
 11 current excursions observed for the insulating macrocapillaries are material-dependent.

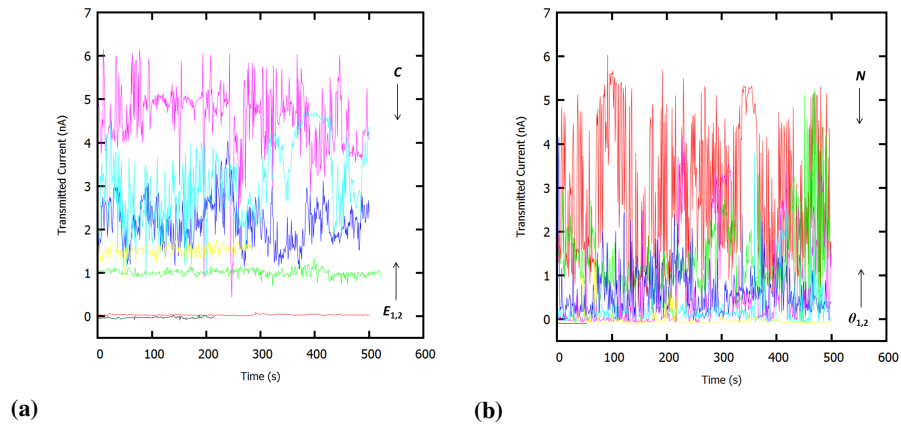


Figure 4: [Color Online] a) Position- and b) angle-dependent raw data for an insulating capillary (Sample # 2,  $l=3.55$  cm,  $d_{in}=d_{out}=0.54$  cm). The transmitted current is plotted as a function of time at varying positions and angles. See text for details.

12 Figure 5 shows the maximum, minimum and mean transmitted ion beam currents

1 along with the calculated geometric transmission from Eqn. 1 as a function of the cor-  
 2 responding tilt angles for the glass macrocapillary data shown in Fig. 4b. The angular  
 3 spread for the maximum transmission is consistent with that predicted for geometric  
 4 transmission. However, the angular spread for minimum, maximum and mean trans-  
 5 mitted ion beam currents differs significantly. This can be seen by examining the criti-  
 6 cal angles for the maximum and minimum cases:  $(\theta_{c,min}, \theta_{c,max}) = (8.65^\circ, 2.83^\circ)$ .

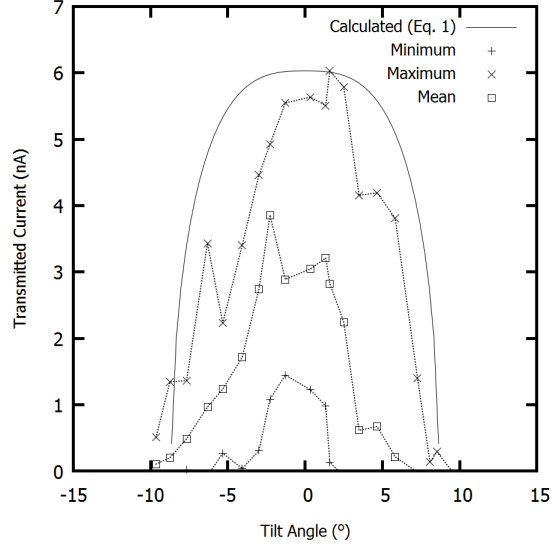


Figure 5: Maximum, mean and minimum of transmitted current as a function of varying tilt angle for an insulating capillary (Sample # 2,  $l=3.55$  cm,  $d_{in}=d_{out}=0.54$  cm). The solid line shows the expected geometrical transmission from the capillary as a function of tilt angle, while the dashed lines are drawn to guide the eye.

7 In order to understand the results of Fig. 5, we first constrain our discussion to two  
 8 angular ranges:  $(\theta < \theta_{c,min})$  and  $(\theta_{c,min} < \theta < \theta_{c,max})$ . Within the first of these  
 9 ranges, we see that the minimum transmitted current is always non-zero. Therefore,  
 10 we can interpret this as a region where ions are always transmitted regardless of time-  
 11 dependent effects, *e.g.* charging of the walls. In the second angular range, we see that  
 12 the minimum transmitted current is always zero, which implies that a time-dependent  
 13 blocking of ion transmission is occurring. This variation or equivalently oscillation in  
 14 the beam transmission may be linked to charge patch formation on the inside walls of  
 15 the macrocapillary. It is well known that electric fields produced by charge patches  
 16 can significantly affect the flight path of the ions. Similar oscillations in transmitted  
 17 currents have been observed for glass macrocapillaries[26], teflon macrocapillaries[27]  
 18 and also for transmission through glass parallel plates [28]. In this context, our data  
 19 indicate a preferential deflection of ions that pass closer to the walls as compared to  
 20 the center of the capillary. That is, ions passing closest to the center of the capillary are not  
 21 subjected to a deflection from electric fields originating from the capillary walls suffi-  
 22 cient to make them escape detection. Conversely, those ions that are not near the center  
 23 are more deflected such that they fall outside the range of detection and the minimum



1 current falls to zero[29]. For the maximum transmitted current data shown in Fig. 5, we  
 2 can interpret it as indicative of the time during which the walls of the macrocapillary  
 3 have discharged and the deflection forces are no longer present. The similarities be-  
 4 tween these data and the metallic macrocapillary result (Fig. 2) then become obvious,  
 5 as both are governed primarily by the geometric constraints of Eqn. 1.

6 Although our data qualitatively point to beam deflection due to charge patch forma-  
 7 tion as the underlying origin of the observed oscillations of transmitted currents in  
 8 insulating macrocapillaries, it is instructive to examine the order of magnitude of the  
 9 fields required to give rise to it within our parameter space. Specifically, the kinetic  
 10 energy of our incident ions is fixed at 1 keV, the path length to the Faraday cup detector  
 11 is 15 cm, and the size of the detector is 2.54 cm. The distance and size of the detector  
 12 together with the velocity of the ions set a constraint on the minimum electric field  
 13 required to deflect the ions outside the detector's acceptance angle. For ions passing  
 14 along the capillary axis, this electric field is calculated to be  $\sim 10$  kV/m. The time taken  
 15 to form such an electric field, assuming no discharge, is on the order of 1 second for  
 16 the incident flux of our beam, which agrees well with the time period of our observed  
 17 oscillations. Transport simulations utilizing classical phase-space dynamics for beam  
 18 deflection along with temporal and spatial charge patch evolution are necessary for a  
 19 detailed quantitative picture[30] of guiding; however, our calculation is sufficient to  
 20 show that charge patch formation can give rise to our observed results.

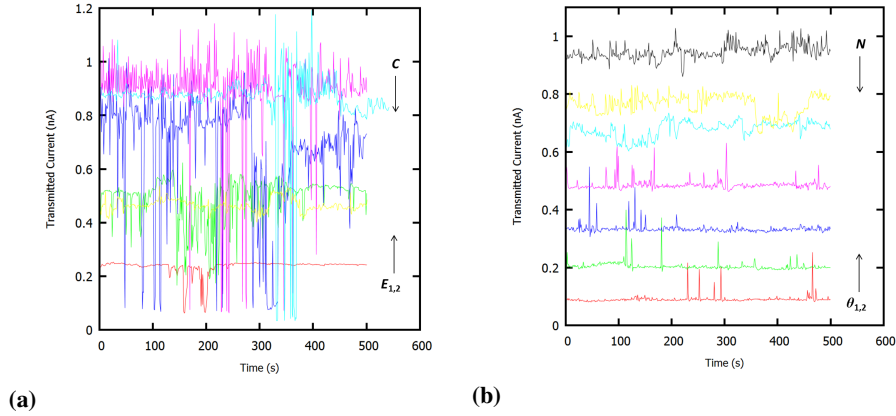


Figure 6: [Color Online] a) Position- and b) angle-dependent raw data for the conical capillary (Sample # 4,  $l=1.96$  cm,  $d_{in}=0.54$  cm,  $d_{out}=0.23$  cm). The transmitted current is plotted as a function of time at varying positions and angles. See text for details.

21 Figure 6 shows the transmitted currents as a function of time for the conical insu-  
 22 lating macrocapillary (Sample # 4) where, as before, Figs. 6a and 6b show the position-  
 23 and angle-dependent data, respectively. The oscillations in the transmitted ion current  
 24 as a function of position are qualitatively similar to those seen in the straight insulat-  
 25 ing capillaries (Samples #2 and #3). The oscillations in the transmitted current as a  
 26 function of angle, however, are significantly smaller in amplitude as compared to both  
 27 the position-dependent transmission of the conical capillary itself and to the straight

1 insulating capillaries in general. As a consequence, the maximum, mean and minimum  
 2 of the transmitted current for the conical insulating macrocapillary appear much closer  
 3 to each other, as shown in Fig. 7. We note that we have used the average radius for  
 4 the calculated transmitted current as opposed to using a more general form of Eq. 1.  
 5 The smaller amplitude of oscillation, or decreased variation in the maximum and mini-  
 6 mum transmitted currents, indicates that charging effects were less pronounced for this  
 7 macrocapillary.

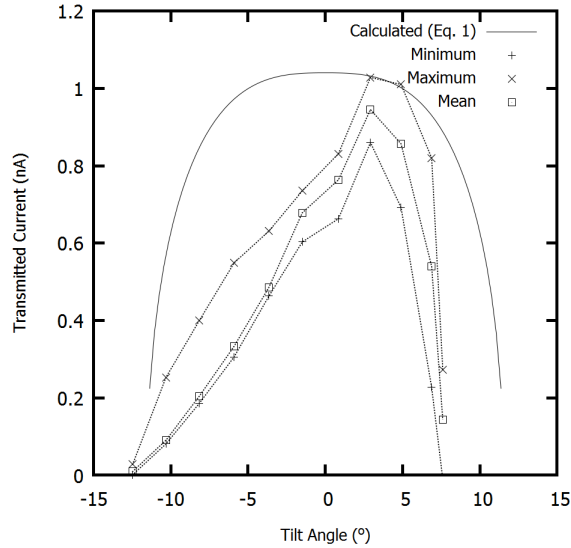


Figure 7: Maximum, mean and minimum of transmitted current as a function of varying tilt angle for the conical insulating capillary (Sample # 4,  $l=1.96$  cm,  $d_{in}=0.54$  cm,  $d_{out}=0.23$  cm). The solid line shows the expected geometrical transmission from the capillary as a function of tilt angle, while the dashed lines are drawn to guide the eye.

#### 8 4. Summary

9 We have measured the position- and angle-dependent transmission characteristics  
 10 of 1 keV  $Rb^+$  ions through metallic and insulating macrocapillaries. Transmission  
 11 through the metal capillary was constant over time and no oscillations were observed  
 12 in the recorded signal. The position-dependent data were used to calculate the beam  
 13 width and also served to verify the stability of the beam over the duration of the exper-  
 14 iment. The measured critical angles for transmission agreed well with those calculated  
 15 from the geometry of the metal capillary, which implies that transmission through the  
 16 capillary was consistent with straight-through line-of-sight transmission. For the insu-  
 17 lating capillaries, the transmitted current was not constant and significant oscillations  
 18 were observed that were absent in the case of the metal capillary. For a range of angles  
 19 consistent with ion transmission parallel to the capillary axis, non-zero transmission  
 20 was always observed; however, outside of this range (but within the geometrical criti-  
 21 cal angle) the transmission fell to zero intermittently. These observations indicate that

1 electric fields due to charge patch formation preferentially deflect ions that are near the  
2 walls of the insulating macrocapillary. The absence of oscillations for the metal macro-  
3 capillary is consistent with this conclusion. In addition, a straightforward calculation  
4 involving the physical parameters of the setup shows that electric fields necessary to de-  
5 flect the ions beyond the acceptance angle of the detector can form within the timescale  
6 of the observed oscillations.

## 7 **Acknowledgments**

8 The authors gratefully acknowledge financial support from the National Science  
9 Foundation (NSF-DMR-0960100), DARPA (ARO Grant No. W911NF-13-1-0042)  
10 and the Clemson University College of Engineering and Science. REU support for  
11 L.A.M. Lyle was provided by the National Science Foundation (NSF-EEC-1262991).

- 12 [1] T. Schenkel, A. V. Barnes, T. R. Niedermayr, M. Hattass, M. W. Newman, G. A.  
13 Machicoane, J. W. McDonald, A. V. Hamza, D. H. Schneider, Deposition of Po-  
14 tential Energy in Solids by Slow, Highly Charged Ions, *Phys. Rev. Lett.* 83 (1999)  
15 4273–4276.
- 16 [2] J. M. Pomeroy, A. C. Perrella, H. Grube, J. D. Gillaspay, Gold nanostructures  
17 created by highly charged ions, *Phys. Rev. B* 75 (2007) 241409.
- 18 [3] F. Aumayr, S. Facsko, A. S. El-Said, C. Trautmann, M. Schleberger, Single ion  
19 induced surface nanostructures: a comparison between slow highly charged and  
20 swift heavy ions, *Journal of Physics: Condensed Matter* 23 (39) (2011) 393001.
- 21 [4] R. E. Lake, J. M. Pomeroy, H. Grube, C. E. Sosolik, Charge State Dependent  
22 Energy Deposition by Ion Impact, *Phys. Rev. Lett.* 107 (2011) 063202.
- 23 [5] D. D. Kulkarni, R. E. Shyam, D. B. Cutshall, D. A. Field, J. E. Harriss, W. R. Har-  
24 rell, C. E. Sosolik, Tracking subsurface ion radiation damage with metal-oxide-  
25 semiconductor device encapsulation, *Journal of Materials Research* 30 (2015)  
26 1413–1421.
- 27 [6] T. Meguro, A. Hida, M. Suzuki, Y. Koguchi, H. Takai, Y. Yamamoto, K. Maeda,  
28 Y. Aoyagi, Creation of nanodiamonds by single impacts of highly charged ions  
29 upon graphite, *Applied Physics Letters* 79 (23) (2001) 3866–3868.
- 30 [7] J. D. Gillaspay, First results from the EBIT at NIST, *Physica Scripta* 1997 (T71)  
31 (1997) 99.
- 32 [8] R. E. Marrs, Recent results from the EBIT and super EBIT at Lawrence Liver-  
33 more National Laboratory, *Physica Scripta* 1997 (T73) (1997) 354.
- 34 [9] F. Meyer, M. Bannister, D. Dowling, J. Hale, C. Havener, J. Johnson, R. Juras,  
35 H. Krause, A. Mendez, J. Sinclair, A. Tatum, C. Vane, E. B. Musafiri, M. Fogle,  
36 R. Rejoub, L. Vergara, D. Hitz, M. Delaunay, A. Girard, L. Guillemet, J. Chartier,  
37 The ORNL multicharged ion research facility upgrade project, *Nuclear Instru-  
38 ments and Methods in Physics Research Section B: Beam Interactions with Ma-  
39 terials and Atoms* 242 (1-2) (2006) 71 – 78.

- 1 [10] E. Galutschek, R. Trassl, E. Salzborn, F. Aumayr, H. Winter, Compact 14.5 GHz  
2 all-permanent magnet ECRIS for experiments with slow multicharged ions, *Journal of Physics: Conference Series* 58 (1) (2007) 395.  
3
- 4 [11] G. Zschornack, S. Landgraf, F. Grossmann, U. Kentsch, V. Ovsyannikov,  
5 M. Schmidt, F. Ullmann, Dresden EBIT: The next generation, *Nuclear Instruments and Methods in Physics Research Section B: Beam Interactions with Materials and Atoms* 235 (1-4) (2005) 514 – 518.  
6  
7
- 8 [12] A. J. G. Martínez, J. R. C. López-Urrutia, D. Fischer, R. S. Orts, J. Ullrich, The  
9 Heidelberg EBIT: Present Results and Future Perspectives, *Journal of Physics: Conference Series* 72 (1) (2007) 012001.  
10
- 11 [13] Y. Fu, K. Yao, B. Wei, D. Lu, R. Hutton, Y. Zou, Overview of the Shanghai EBIT,  
12 *Journal of Instrumentation* 5 (08) (2010) C08011.
- 13 [14] H. Watanabe, F. Currell, The Belfast EBIT, *Journal of Physics: Conference Series*  
14 2 (1) (2004) 182.
- 15 [15] R. Shyam, D. D. Kulkarni, D. A. Field, E. S. Srinadhu, D. B. Cutshall, W. R.  
16 Harrell, J. E. Harriss, C. E. Sosolik, First multicharged ion irradiation results  
17 from the CUEBIT facility at Clemson University, *AIP Conference Proceedings*  
18 1640 (1) (2015) 129–135.
- 19 [16] D. Medlin, W. Heffron, A. Siegel, K. Wilson, A. Klingenberger, A. Gall,  
20 M. Rusin, D. Dean, E. Takacs, Development of an x-ray irradiation port for  
21 biomedical applications at the CUEBIT facility, *Journal of Physics: Conference Series* 583 (1) (2015) 012048.  
22
- 23 [17] N. Stolterfoht, J.-H. Bremer, V. Hoffmann, R. Hellhammer, D. Fink, A. Petrov,  
24 B. Sulik, Transmission of 3 keV  $\text{Ne}^{7+}$  Ions through Nanocapillaries Etched  
25 in Polymer Foils: Evidence for Capillary Guiding, *Phys. Rev. Lett.* 88 (2002)  
26 133201.
- 27 [18] C. Lemell, J. Burgdörfer, F. Aumayr, Interaction of charged particles with insu-  
28 lating capillary targets - The guiding effect, *Progress in Surface Science* 88 (3)  
29 (2013) 237 – 278.
- 30 [19] See Sec. 2.2 in Reference [18].
- 31 [20] A. Wartak, R. Bereczky, G. Kowarik, K. Tksi, F. Aumayr, Conceptual design and  
32 sample preparation of electrode covered single glass macro-capillaries for study-  
33 ing the effect of an external electric field on particle guiding, *Nuclear Instruments and Methods in Physics Research Section B: Beam Interactions with Materials and Atoms* 354 (2015) 324 – 327, 26th International Conference on Atomic Collisions in Solids.  
34  
35  
36
- 37 [21] E. Giglio, R. DuBois, A. Cassimi, K. Tksi, Low energy ion transmission through  
38 a conical insulating capillary with macroscopic dimensions, *Nuclear Instruments and Methods in Physics Research Section B: Beam Interactions with Materials*  
39

- 1 and Atoms 354 (2015) 82 – 85, 26th International Conference on Atomic Colli-  
2 sions in Solids.
- 3 [22] T. M. Kojima, T. Ikeda, Y. Kanai, Y. Yamazaki, Ion guiding in curved glass cap-  
4 illaries, Nuclear Instruments and Methods in Physics Research Section B: Beam  
5 Interactions with Materials and Atoms 354 (2015) 16 – 19, 26th International  
6 Conference on Atomic Collisions in Solids.
- 7 [23] M. P. Ray, R. E. Lake, S. A. Moody, V. Magadala, C. E. Sosolik, A hyperthermal  
8 energy ion beamline for probing hot electron chemistry at surfaces, Rev. Sci. Instr.  
9 79 (2008) 076106.
- 10 [24] M. Menzinger, L. Wåhlin, High Intensity, Low Energy Spread Ion Source for  
11 Chemical Accelerators, Review of Scientific Instruments 40 (1) (1969) 102–105.
- 12 [25] See Figure 1 in reference [23].
- 13 [26] M. Alshammari, K. Alshammari, A. Cudd, R. DuBois, K. Tksi, Exploring new  
14 aspects and practical applications of capillary guiding of charged particle beams,  
15 Nuclear Instruments and Methods in Physics Research Section B: Beam Interac-  
16 tions with Materials and Atoms 354 (2015) 20 – 22, 26th International Conference  
17 on Atomic Collisions in Solids.
- 18 [27] T. M. Kojima, T. Ikeda, Y. Kanai, Y. Yamazaki, V. A. Esaulov, Ion beam guiding  
19 with straight and curved Teflon tubes, Journal of Physics D: Applied Physics  
20 44 (35) (2011) 355201.
- 21 [28] T. Ikeda, Y. Iwai, T. M. Kojima, S. Onoda, Y. Kanai, Y. Yamazaki, Resistive  
22 switching induced on a glass plate by ion beam irradiation, Nuclear Instruments  
23 and Methods in Physics Research Section B: Beam Interactions with Materials  
24 and Atoms 287 (2012) 31 – 34.
- 25 [29] E. Gruber, G. Kowarik, F. Ladinig, J. P. Wacławek, D. Schrempf, F. Aumayr,  
26 R. J. Berezsky, K. Tórkési, P. Gunacker, T. Schweigler, C. Lemell, J. Burgdörfer,  
27 Temperature control of ion guiding through insulating capillaries, Phys. Rev. A  
28 86 (2012) 062901.
- 29 [30] See Sec. 4 in Reference [18].